# ACS OMEGA

Article

# Detecting *Escherichia coli* Biofilm Development Stages on Gold and Titanium by Quartz Crystal Microbalance

Rosa Ripa, Amy Q. Shen, and Riccardo Funari*

Read Online

ACCESS | Metrics & More | Article Recommendations

**ABSTRACT:** Bacterial biofilms are responsible for persistent infections and biofouling, raising serious concerns in both medical and industrial processes. These motivations underpin the need to develop methodologies to study the complex biological structures of biofilms and prevent their formation on medical implants, tools, and industrial apparatuses. Here, we report the detailed comparison of *Escherichia coli* biofilm development stages (adhesion, maturation, and dispersion) on gold and titanium surfaces by monitoring the changes in both frequency and dissipation of a quartz crystal microbalance (QCM) device, a cheap and reliable microgravimetric sensor which allows the real-time and label-free characterization of various stages of biofilm development. Although gold is the most common electrode material used for QCM sensors, the titanium electrode is also readily available for QCM sensors; thus, QCM sensors with different metal electrodes serve as a simple platform to probe how pathogens interact with different metal substrates. The QCM outcomes are further confirmed by atomic force microscopy and crystal violet staining, thus validating the effectiveness of this surface sensitive sensor for microbial biofilm research. Moreover, because QCM technology can easily modify the substrate types and coatings, QCM sensors also provide well-controlled experimental conditions to study antimicrobial surface treatments and eradication procedures, even on mature biofilms.
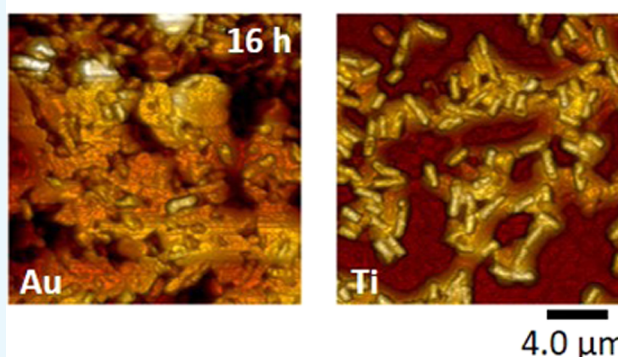
## 1. INTRODUCTION

Bacteria manifest two modes of growth: planktonic, where the cells are free to move in a liquid environment, and biofilm, in which the cells grow onto a surface in a sessile state.[1,2] In the latter form, the microorganisms are closely packed on a solid surface within a self-produced matrix of extracellular polymeric substances (EPSs). This viscoelastic scaffold constituted of proteins and polysaccharides provides many structural and functional benefits such as improved resources capture, adhesion to surfaces, digestive capacity, protection against external agents, and prevention of bacterial dehydration. Furthermore, the EPS matrix facilitates intercellular interactions and horizontal gene transfer.[3] Another key feature of bacterial biofilms concerns the development of their peculiar resistance against antimicrobial agents.[4] This leads to persistent infections in humans because of the contamination of medical devices,[5] biofouling and corrosion problems in industrial settings,[6,7] and major issues in wastewater treatments,[8] which contribute to the rise of health care costs and economic losses. Moreover, bacterial biofilms can be found on most surfaces in the environment, whether natural[9,10] or synthetic materials.[2,5] Therefore, the significance of biofilms has motivated ongoing research efforts to understand the mechanism of biofilm formation and to select and/or engineer more efficient antimicrobial surfaces.[11]

Biofilm formation is a dynamic and complex physiological process involving different development stages[12−14] (Figure 1), which should be considered when designing strategies for biofilm treatments. First, the planktonic cells approach the surface, where a conditioning layer is formed. This layer is composed of organic and inorganic molecules that are either secreted by the cells nearby the surface or settled from the bulk solution. Interactions between the bacteria and the conditioning layer can facilitate microbial adhesion. Consequently, physical interactions and bacterial appendages allow the planktonic cells to adhere onto the surface (early adhesion). As soon as the adhesion becomes irreversible, bacteria start multiplying, forming clusters and producing EPS, thus losing their motility and forming the initial biofilm (step 1 in Figure 1). The biofilm grows until it reaches its maximum thickness, thus achieving the maturation stage (step 2 in Figure 1). As
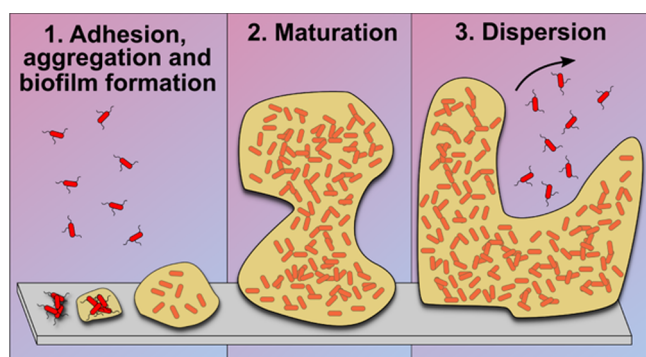
**Figure 1.** Stages of biofilm development. Bacteria appendages, such as curli, drive cell adhesion onto solid surfaces (step 1). This interaction is stabilized by the production of EPSs, which improve the attachment and offer both mechanical and chemical protection for the bacteria. Biofilm growth and maturation (step 2) is followed by the release of free-floating bacteria for further colonization (step 3).

soon as the biofilm reaches a critical mass, it starts to disperse planktonic cells (step 3 in Figure 1). This dispersion process allows bacteria to swim back into the bulk liquid for colonizing new surfaces.

Traditional biofilm research focused their attention on biofilms formed on conventional surfaces, such as steel,[15] plastic,[16] glass[17] surfaces in test tubes, 96-well plates,[18] or flow cells.[19] In particular, there is an increasing interest in the selection, design, and production of novel antimicrobial surfaces to prevent biofilm-associated infections[20−22] and biofouling.[23,24] For instance, Pappas et al.[25] succeeded in killing almost 70% of a population of *Staphylococcus aureus* and *Escherichia coli* by using a temperature-responsive polymeric surface.

Several new methodologies have been developed or adapted to biofilm studies.[26−28] Microtiter plate,[29] Calgary device,[30] and the biofilm ring test[31] provide high-throughput studies, but they do not offer real-time investigation during the biofilm development stages. Flow chambers[32,33] and microfluidic[34,35] systems allow the formation of the biofilm in situ with real-time monitoring by optical detection methods,[36] thus requiring the use of additional instrumentation. In addition, the common microscopic techniques applied to study biofilms [i.e., scanning electron microscopy (SEM),[37] atomic force microscopy (AFM),[38] and transmission electron microscopy (TEM)[39]] are time-consuming and expensive. Among these techniques, quartz crystal microbalance (QCM) is a cost-effective and reliable technology for bacterial biofilm studies. In fact, QCM has received increasing attention because of its flexibility in investigating molecular recognition and surface phenomena.[40,41] In particular, QCM can measure mass deposition/adsorption with a resolution of ≈1 ng/Hz, monitor changes in the stiffness of materials adsorbed on the QCM sensor surface,[42] and track various biological processes involving DNA hybridization,[43,44] antigen−antibody binding,[45,46] and prokaryotic and eukaryotic cell adhesion responses to different stimuli.[47,48] More recently, QCM has been used as a sensor platform to study the biofilm adhesion,[49−51] the physiological and genetic factors related to biofilm formation,[52] and the effect of flow conditions over bacterial cells.[53] In addition, the QCM sensing surface can be easily functionalized with different types of materials.[54−56] Specifically, Reipa et al.[57] combined the QCM device with reflectance measurements to track the formation of the biofilm of the bacterium

*Pseudomonas aeruginosa* on the gold sensor surface. They verified the presence of a mature biofilm by confocal and fluorescence microscopy at the end of the experiment. However, the reflectance measurements suffered from solution turbidity and biofilm inhomogeneity. Another QCM-based approach to capture the stages of biofilm formation of the bacterium *Pseudomonas putida* was developed by Sprung et al.[58] In this work, biofilm formation was tracked on either a pristine (i.e., clean gold) or a modified (i.e., Lipodex E, concanavalin A, or phenanthrene) gold sensor surface. However, independent validation of the presence and status of the biofilm using other methods (e.g., microscopy and microbiological techniques) was not provided. Recently, Amer et al.[59] developed a custom QCM multichannel system to improve the accuracy of the QCM measurement with different bacteria. However, detailed information on various biofilm development stages was missing. All these aspects were recently reviewed by Alexander et al.,[60] with extensive discussions on the factors affecting bacterial adhesion and biofilm formation, modifications of the QCM gold sensor surface, and modelling of the QCM response.

The interaction between bacteria and the surface they interact with has critical implications in biofouling and infections. For this reason, it is important to develop reliable and flexible methodologies to study biofilm formation on a wide range of materials. Since the antimicrobial resistance of bacterial biofilms is a time-dependent property,[61−64] real-time analysis performed at high temporal resolution can shed new insights to understand biofilm formation and identify optimal eradication treatments. Because QCM offers both these advantages, in the present work, we focused on the use of this technology to characterize *E. coli* biofilm formation in real time on two typical metal surfaces: gold and titanium. Most of the existing work of using QCM to study biofilm involves gold-based electrodes. Indeed, gold is the most common metal used for QCM sensors[41] and has the advantages of easy surface modification. Nevertheless, the electrode of the metal/quartz resonators can be directly incorporated in the QCM device to track biofilm growth under conditions resembling real environments. Therefore, in this work, we investigated biofilm formation not only on gold but also on titanium surfaces as titanium has been widely used in implantable devices because of its corrosion-resistant nature and biocompatibility.[65]

In this work, *E. coli* biofilm development stages are investigated directly on the QCM surface by monitoring the sensor resonant frequency and energy dissipation signals for ≈24 h. Differences in terms of morphology and biomass between the biofilms grown on gold and titanium electrodes are measured and confirmed by AFM and crystal violet (CV) staining outputs. Finally, QCM technology can be easily extended to other bacteria types and materials, thus providing a general tool to investigate biofilm formation in real time.

## 2. RESULTS AND DISCUSSION

QCM is used to track *E. coli* biofilm formation and identify its development stages on gold and titanium surfaces. The morphology of the formed biofilm is then characterized by AFM directly on the metal sensor surface. Finally, both QCM and AFM results are verified through the CV assay, a standard microbiological staining technique used to evaluate biofilm biomass.

**2.1. Real-Time Observation of *E. coli* Biofilm Development Stages on Gold and Titanium Substrates.** QCM
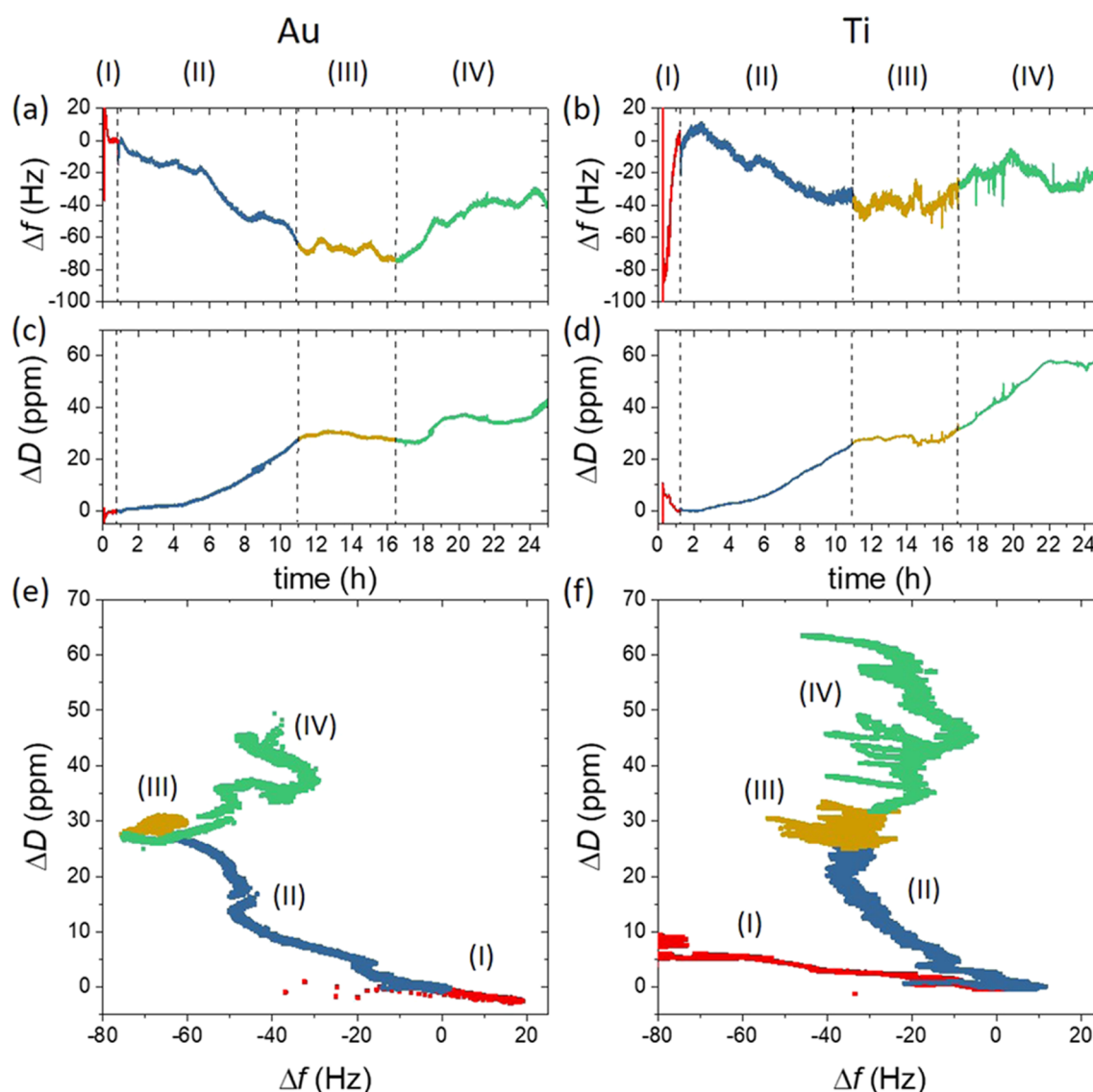
**Figure 2.** QCM sensorgrams of *E. coli* growing on gold (a,c) and titanium (b,d). The color scheme highlights the stages of the experiment: initial stabilization with culture medium [red, (I)], biofilm formation [blue, (II)], maturation [yellow, (III)], and release of free planktonic cells [green, (IV)]. (e,f) Panels show the dissipation vs frequency plots for measurements performed on gold and titanium, respectively.

with dissipation monitoring (QCM-D) allows to measure both the resonant frequency of the oscillating quartz and the energy dissipation associated with the material adsorbed on the sensor surface.[41] Whereas negative changes in the resonant frequency usually indicate an addition of mass on the QCM, an increase in the energy dissipation is related to a reduction in the stiffness of the material in contact with the sensor surface.

The QCM sensorgrams started recording when the *E. coli* culture is set directly on the metal sensor surface (Figure 2). Various phases of the biofilm development can be distinguished based on the frequency and dissipation values captured in the sensorgram, with the focus on the data obtained 1 h after the culture medium was loaded in the QCM chamber (vertical dashed line at the end of the red data in Figure 2a−d).

Figure 2 illustrates the QCM sensorgrams of *E. coli*'s growth on both gold and titanium sensors. For the gold-based QCM measurements (Figure 2a,c), the sensor signals are stabilized in lysogeny broth (LB) [red data, (I)] before loading the inoculum (vertical dashed lines at about 1 h). This leads to

bacterial adhesion and growth on the QCM electrode (see stage 1 in Figure 1), which results in a progressive decrease in frequency and increase in dissipation followed by signal stabilization at about 11 h [blue data, (II)]. This behavior reflects the formation of a soft layer of bacteria and EPS on the sensor surface. Both frequency and dissipation signals remain stable for the next ≈6 h [yellow data, (III)], meaning that the biofilm reached its maturation, and the viscoelasticity properties of the attached layer remain unchanged. Next, at ≈17 h, bacteria start to be released in the liquid phase,[1] causing a mass loss and an increase in the viscoelasticity of the biofilm, which corresponds to the increase of both resonant frequency and dissipation energy in the QCM sensorgram [green data, (IV)]. At the end of the measurement, at ≈24 h after the loading of the inoculum, the QCM sensor reaches final values of $\Delta f$ and $\Delta D$ of $-34 \pm 5$ Hz and $40 \pm 12$ ppm, respectively.

Similar phases [i.e., incubation with LB in red, (I); biofilm formation in blue, (II); maturation in yellow, (III); dispersion in green, (IV)] can be observed on the titanium substrate (Figure 2b,d). However, the overall frequency variation on
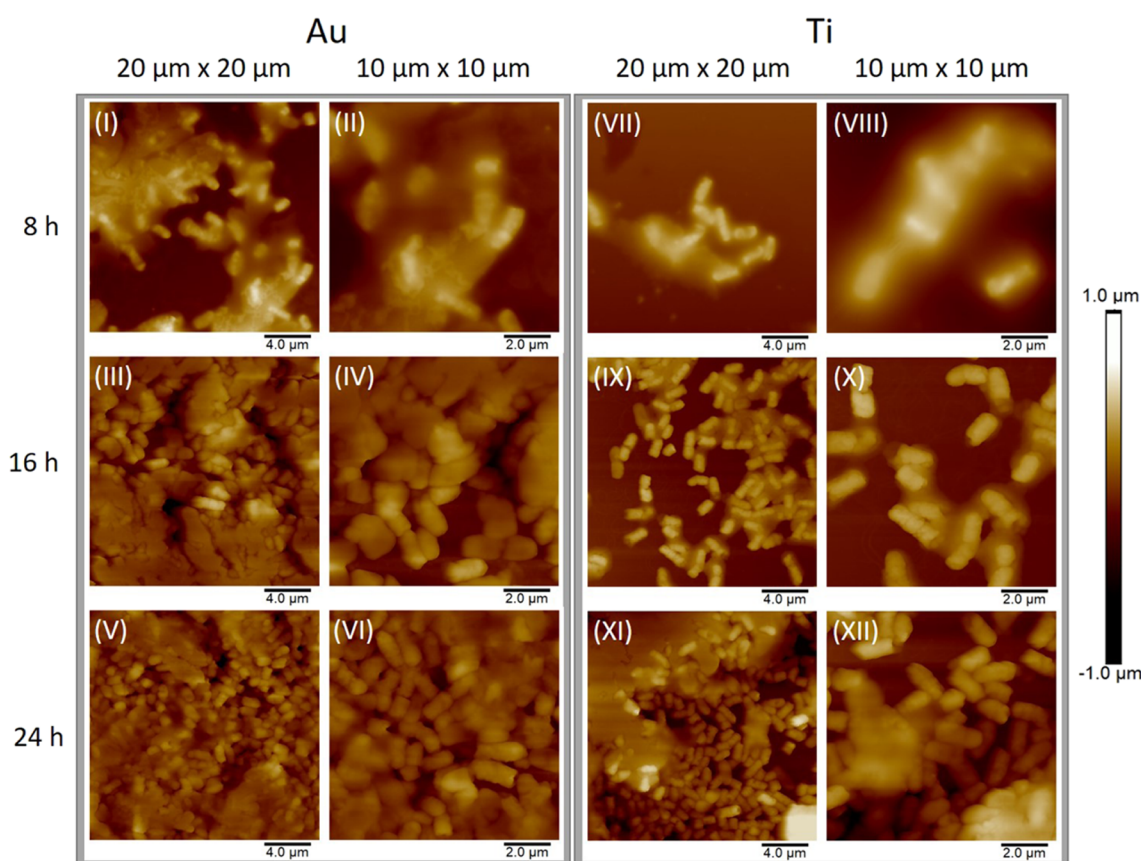
**Figure 3.** High-resolution AFM images of *E. coli* biofilm on gold (left panels) and titanium (right panels) QCM electrodes at different growth times. The rows show the progressive magnification of the bacterial biofilm (20 $\mu$m × 20 $\mu$m and 10 $\mu$m × 10 $\mu$m areas, respectively) after 8, 16, and 24 h from the loading of the inoculum.

titanium is smaller but with larger noise than the one obtained on gold (the final $\Delta f$ value is −13 ± 14 Hz). On the other hand, the dissipation signal exhibits similar profiles on both gold- and titanium-based QCMs until the biofilm reaches the maturation phase [yellow data, (III)]. Subsequently, in the last stage, the dissipation signal reaches much larger values on titanium (the final $\Delta D$ value is 68 ± 19 ppm) in comparison to the values on the gold electrode ($\Delta D$ 40 ± 12 ppm). Our observations suggest that the *E. coli* biofilm formed on titanium is less abundant and more viscoelastic than those produced on gold. The comparison of the QCM sensorgrams with two different substrate materials shows that QCM is able to distinguish the effects of different materials on biofilm formation. Further confirmation can be seen by the dissipation versus frequency plots (*Df* plots shown in Figure 2e,f for gold and titanium, respectively). In these graphs, the $\Delta D/\Delta f$ ratio highlights the structural properties of the biofilm attached on the QCM. Briefly, a larger $\Delta D/\Delta f$ value corresponds to a more viscoelastic film attached to the surface.

The incubation of the gold surface with LB [red data, (I) in Figure 2e,f] produces a compact layer on the QCM, which causes, on both Au and Ti, a significant change in frequency but minor variations in dissipation. On the other hand, all three phases of the biofilm development (II, III, and IV, shown in blue, yellow, and green, respectively in Figure 2e,f) produce a much steeper trend on titanium, indicating that the biofilm formed on Ti is softer than that produced on Au.

**2.2. Morphological Characterization of *E. coli* Biofilm via AFM and Biomass Estimation Using CV Assay.** After

*E. coli* have grown on QCM gold and titanium electrodes for 8, 16, and 24 h, the resulting microbial biofilms are imaged by an atomic force microscope operating in the tapping mode. The high spatial resolution offered by AFM allows not only to image the single cells constituting the biofilm but also to identify the contribution of the EPS matrix. Such a detailed and time-dependent morphological characterization is missing in many papers focusing on the use of QCM for biofilm study. Indeed, this technique has proven to be extremely useful for characterizing the bacterial biofilm morphology, bacterial interactions, and attachment on surfaces.[66] Therefore, we used AFM images to correlate the biofilm structure at specific times with the stages highlighted by the QCM sensorgrams. Growth and development of *E. coli* biofilms on gold and titanium QCM electrodes are reported in Figure 3.

The high-resolution images clearly show the biofilm development stages both on gold and titanium. At 8 h (panels I, II, VII, and VIII), the bacteria adhere onto the metal surfaces, start to aggregate, and produce EPS, leading to biofilm formation. On gold (panels I and II), more than half of the QCM gold electrode is already covered by bacteria and EPS. On the other hand, only fewer bacteria adhere on the titanium surface (panels VII and VIII), with a consequential lower amount of EPS surrounding the microbial cells. At 16 h (panels III, IV, IX, and X), the biofilms approach the maturation stage. In particular, on gold (panels III and IV), we can clearly see the compact structure constituted of bacteria and EPS. At the same time, on titanium (panels IX and X), only ≈50% of the surface is covered by cells and EPS. Finally,

at 24 h (panel V, VI, XI, and XII), both single cells in rod-shapes and biofilms are captured in the image, meaning that the biofilm has reached the final dispersion stage by releasing free-floating bacteria. On titanium, even though some areas present a completely formed biofilm at 24 h (top left area in panel XI), the titanium surface is not completely covered by the bacteria. These observations imply that *E. coli* has higher affinity for gold than titanium.

Additional verification of the QCM results is obtained by the CV assay. This staining procedure is one of the most common techniques used to measure cell biomass and is routinely used to study biofilm formation. Unfortunately, the fact that CV is a disruptive assay strongly limits its use for time-dependent characterizations. In this technique, the biofilm biomass is estimated by measuring the absorbance of the stained sample at 570 nm. The greater the biofilm mass, the higher the absorbance signal. We used the CV assay to measure the biofilm's biomass after 24 h of bacterial growth on the gold and titanium QCM surfaces and on the plastic substrate of a 96-well microtiter plate, which we used as the reference material. The results of the CV staining are shown in Figure 4.
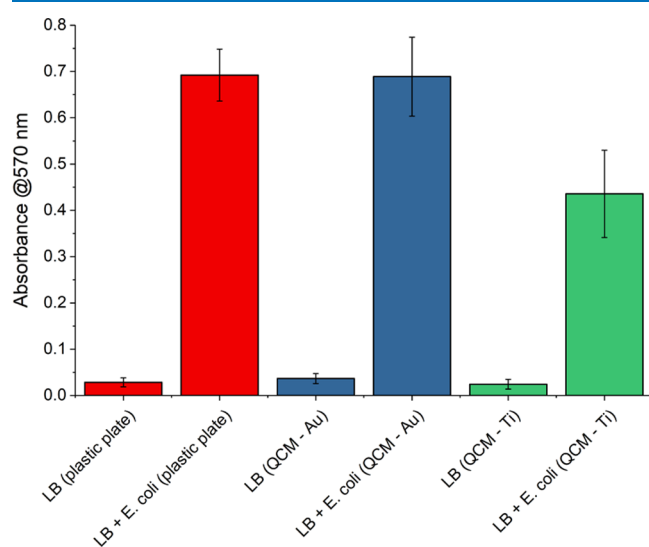


**Figure 4.** CV assay for *E. coli* grown on three different surfaces: plastic (red), gold (blue), and titanium (green). In all these tests, bacteria are grown for 24 h before staining. While *E. coli* reaches mostly the same biomass on both plastic (reference) and gold, the bacteria produces a smaller biofilm on titanium.

The absorbance of sterile culture medium (LB, used as background) is almost the same on plastic ($0.03 \pm 0.01$), gold ($0.04 \pm 0.01$), and titanium ($0.02 \pm 0.01$). After 24 h, the biomass of the *E. coli* biofilm on the gold electrode ($0.69 \pm 0.05$) is similar to the one reached on the plastic plate ($0.69 \pm 0.06$), which is used as a reference surface. On the other hand, the biofilm produced on the titanium surface is less massive ($0.44 \pm 0.09$). The CV results are consistent with the QCM measurements, confirming the higher affinity of *E. coli* for gold over titanium substrates.

## 3. CONCLUSIONS

In this paper, we demonstrate that QCM devices provide a cheap and reliable alternative to conventional microbiological techniques to study stages of biofilm formation in real-time with high temporal resolution, without the need of any labelling or disrupting procedure. The QCM results are in good agreement with the high-resolution imaging provided by AFM as well as with the outcomes of the conventional CV staining technique, thus confirming the reliability of the surface sensitive device used in this work.

We show that the QCM system allows the detailed real-time characterization of the stages of bacterial biofilm development on both gold and titanium for more than 24 h, thus proving the effectiveness of this sensing platform in comparative studies on biofilm growth of different materials. We also report that *E. coli* has higher affinity and more abundant biofilm formation on gold sensors in comparison to titanium sensors. Since the QCM surface properties can be easily modulated and the sensor platform can be integrated with microfluidic setups, this technology can offer an enormous range of opportunities for investigating biofilm properties and development, screening for biofilm specific drugs, developing antimicrobial surface treatments, and designing biofilm eradication procedures.

## 4. MATERIALS AND METHODS

**4.1. Bacterial Growth.** *E. coli* (WT MG1655, Lab collection) is streaked on LB agar (Sigma-Aldrich, L3022 and A1296) plates. The stock is kept in glycerol at $-80$ °C. Single colonies are picked from the plates and used to inoculate 20 mL of LB and grown overnight ($\approx 16$ h) at 37 °C under continuous shaking (200 rpm).

**4.2. QCM.** The QCM-D device (openQCM Q-1) is purchased from Novaetech, Italy. Gold-quartz (QL0765) and titanium-quartz (QL0763) oscillators are purchased from IEV, Italy. They are AT-CUT quartz with a fundamental frequency of 10 MHz. The quartz crystal and the metal electrode diameters are 1.37 and 0.6 cm, respectively. The liquid is confined on the quartz oscillator via an open cell that allows sample volumes up to 200 $\mu$L. The cell is closed with a Teflon cover, and the whole sensing modulus is protected by a three-dimensional-printed cap containing a water reservoir. This is critical to prevent sample evaporation. Both resonant frequency and dissipation values are recorded in real time via the manufacturer's software. Data are then analyzed using OriginPro 2017 (OriginLab).

**4.3. Monitoring *E. coli* Biofilm Formation Using QCM.** LB (200 $\mu$L) is loaded into the QCM chamber, and when both the frequency and dissipation signals are stable (it takes about 1 h from the loading of the LB), 1 $\mu$L of the overnight bacterial culture (equal to an initial concentration of bacteria of about $2 \times 10^7$ CFU/mL) is then added to the QCM chamber. Both resonant frequency and dissipation are monitored for 24 h. All measurements are performed in triplicate.

**4.4. Morphological Characterization of Microbial Biofilms via AFM.** Microscopic characterization of *E. coli* biofilms grown on QCM gold and titanium surfaces is performed using an atomic force microscope (Dimension ICON3 from Bruker, Japan) equipped with aluminum back-coated cantilevers (OTESPA-R3, Bruker, Japan) having nominal tip radius values $\approx 7$ nm, spring constant $k \approx 26$ N/m, and resonant frequency $f_0 \approx 300$ kHz. The microbial biofilms are imaged in the tapping mode with a scanning speed of 1 line/s and a relatively high amplitude set-point ratio ($A_{sp}/A_{free} \approx 0.85$) to reduce the risk of tip contamination. Areas of 20 $\mu$m × 20 $\mu$m and 10 $\mu$m × 10 $\mu$m are scanned with a resolution of 512 pixels per line. All measurements are performed in triplicate, and image analysis is performed using NanoScope Analysis 1.8 software (Bruker, USA).

**4.5. CV Staining.** CV assay is a well-established methodology used to quantify the mass of biofilms.[67,68] Most of the existing CV staining protocols require that the bacteria be cultivated on microtiter plates.[69,70] In this work, a custom procedure has been developed to stain the bacteria directly onto the sensor surface to validate the results obtained with the QCM device at the end of 24 h. First, a CV staining solution (0.5%) is prepared by dissolving 0.5 g of CV powder (Sigma-Aldrich, C6158) in 80 mL of distilled water, followed by addition of 20 mL of methanol. The solution is gently mixed to completely dissolve the dye powder. The bacterial biofilm is grown for 24 h in a standalone device consisting of a quartz sensor and the open cell of the QCM device. Growing conditions are similar to those used for growing bacteria on the QCM (wells are filled with 200 $\mu$L of culture medium, and after 1 h, 1 $\mu$L of the overnight culture is loaded). At the same time, as a control, cells are grown under the same conditions in a 96-well plate at room temperature. Each condition is tested five times, and wells containing only the culture medium are used as the background. After 24 h, the exhaust medium is aspirated, and the biofilms are washed twice in a gentle stream of tap water. Then, the plate and the device are inverted on a filter paper and tapped gently to remove any remaining liquid. Next, 100 and 50 $\mu$L of 0.5% CV staining solution are added to the sample well of the customized device and the 96-well plate, respectively. Both the QCM device and the plate are then incubated for 20 min at room temperature on a bench rocker oscillating at 20 rpm. Both electrodes of the QCM device and the plastic substrate in the 96-well plates are washed four times using tap water and then tapped on a filter paper. Both the plate and the device are next air-dried for 24 h at room temperature without lids. A methanol droplet (250 and 125 $\mu$L for device and plate, respectively) is added to each well. Next, both the plate and the QCM device are incubated for 20 min at room temperature on a bench rocker at 20 rpm. Samples in the standalone device are then moved to the multiwell plate. Finally, the absorbance at 570 nm is recorded using an ELISA plate reader (Multiskan GO from Thermo Scientific).

**4.6. QCM Surface Cleaning.** QCM gold-coated quartz substrates are cleaned by using the "piranha solution," a 3:1 mixture of sulfuric acid ($H_2SO_4$) and 30% hydrogen peroxide ($H_2O_2$). Since the piranha solution is a strong oxidizing agent, it is commonly used in microelectronics to remove organic contaminants from substrates. In the fume hood, hydrogen peroxide (Sigma-Aldrich, 216763) is slowly poured in a glass beaker containing sulfuric acid (Sigma-Aldrich, 258105) resulting in an extremely exothermic reaction. After the solution cools, QCM sensor substrates are immersed with steel tweezers in the reactive solution for about 2 min. Next, the substrates are washed with Milli-Q water and dried with a gentle stream of nitrogen. This aggressive chemical treatment allows QCM sensor substrates to be reused up to four times.

Because the piranha solution etches the titanium electrodes, the titanium surfaces are cleaned via sonication in acetone and then isopropanol. Each step takes about 5 min. Finally, similar to the gold electrodes, the titanium surfaces are rinsed with Milli-Q water and dried with a gentle stream of nitrogen.

## ■ AUTHOR INFORMATION

**Corresponding Author**
  **Riccardo Funari** − *Okinawa Institute of Science and Technology Graduate University, Okinawa, Japan;*
    orcid.org/0000-0003-1786-3833;
  Email: riccardo.funari@oist.jp

**Other Authors**
  **Rosa Ripa** − *Okinawa Institute of Science and Technology Graduate University, Okinawa, Japan*
  **Amy Q. Shen** − *Okinawa Institute of Science and Technology Graduate University, Okinawa, Japan;*
    orcid.org/0000-0002-1222-6264

Complete contact information is available at:
https://pubs.acs.org/10.1021/acsomega.9b03540

**Notes**
The authors declare no competing financial interest.

## ■ ACKNOWLEDGMENTS

## ■ REFERENCES

(1) Flemming, H.-C.; Wingender, J.; Szewzyk, U.; Steinberg, P.; Rice, S. A.; Kjelleberg, S. Biofilms: an emergent form of bacterial life. *Nat. Rev. Microbiol.* **2016**, *14*, 563.

(2) Donlan, R. M. Biofilms: microbial life on surfaces. *Emerging Infect. Dis.* **2002**, *8*, 881.

(3) Flemming, H.-C.; Neu, T. R.; Wozniak, D. J. The EPS matrix: the "house of biofilm cells". *J. Bacteriol.* **2007**, *189*, 7945−7947.

(4) Davies, D. Understanding biofilm resistance to antibacterial agents. *Nat. Rev. Drug Discovery* **2003**, *2*, 114.

(5) Donlan, R. M. Biofilm formation: a clinically relevant microbiological process. *Clin. Infect. Dis.* **2001**, *33*, 1387−1392.

(6) Jass, J.; Surman, S.; Walker, J. T. *Industrial Biofouling: Detection, Prevention, and Control*; Wiley, 2000.

(7) Rao, T. S.; Kora, A. J.; Chandramohan, P.; Panigrahi, B. S.; Narasimhan, S. V. Biofouling and microbial corrosion problem in the thermo-fluid heat exchanger and cooling water system of a nuclear test reactor. *Biofouling* **2009**, *25*, 581−591.

(8) Huang, H.; Peng, C.; Peng, P.; Lin, Y.; Zhang, X.; Ren, H. Towards the biofilm characterization and regulation in biological wastewater treatment. *Appl. Microbiol. Biotechnol.* **2019**, *103*, 1115−1129.

(9) Dow, J. M.; Crossman, L.; Findlay, K.; He, Y.-Q.; Feng, J.-X.; Tang, J.-L. Biofilm dispersal in Xanthomonas campestris is controlled by cell−cell signaling and is required for full virulence to plants. *Proc. Natl. Acad. Sci. U.S.A.* **2003**, *100*, 10995−11000.

(10) Costerton, J. W.; Stewart, P. S.; Greenberg, E. P. Bacterial biofilms: a common cause of persistent infections. *Science* **1999**, *284*, 1318−1322.

(11) Gu, H.; Ren, D. Materials and surface engineering to control bacterial adhesion and biofilm formation: A review of recent advances. *Front. Chem. Sci. Eng.* **2014**, *8*, 20−33.

(12) O'Toole, G.; Kaplan, H. B.; Kolter, R. Biofilm formation as microbial development. *Annu. Rev. Microbiol.* **2000**, *54*, 49−79.

(13) Sauer, K.; Camper, A. K.; Ehrlich, G. D.; Costerton, J. W.; Davies, D. G. Pseudomonas aeruginosa displays multiple phenotypes during development as a biofilm. *J. Bacteriol.* **2002**, *184*, 1140−1154.

(14) Garrett, T. R.; Bhakoo, M.; Zhang, Z. Bacterial adhesion and biofilms on surfaces. *Prog. Nat. Sci.* **2008**, *18*, 1049−1056.

(15) Ryu, J.-H.; Beuchat, L. R. Biofilm Formation by Escherichia coli O157:H7 on Stainless Steel: Effect of Exopolysaccharide and Curli Production on Its Resistance to Chlorine. *Appl. Environ. Microbiol.* **2005**, *71*, 247−254.

(16) Prigent-Combaret, C.; Prensier, G.; Le Thi, T. T.; Vidal, O.; Lejeune, P.; Dorel, C. Developmental pathway for biofilm formation in curli-producing Escherichia coli strains: role of flagella, curli and colanic acid. *Environ. Microbiol.* **2000**, *2*, 450−464.

(17) Hammer, B. K.; Bassler, B. L. Quorum sensing controls biofilm formation in Vibrio cholerae. *Mol. Microbiol.* **2003**, *50*, 101−104.

(18) Gonzalez Barrios, A. F.; Zuo, R.; Hashimoto, Y.; Yang, L.; Bentley, W. E.; Wood, T. K. Autoinducer 2 controls biofilm formation in Escherichia coli through a novel motility quorum-sensing regulator (MqsR, B3022). *J. Bacteriol.* **2006**, *188*, 305−316.

(19) Klausen, M.; Heydorn, A.; Ragas, P.; Lambertsen, L.; Aaes-Jørgensen, A.; Molin, S.; Tolker-Nielsen, T. Biofilm formation by Pseudomonas aeruginosa wild type, flagella and type IV pili mutants. *Mol. Microbiol.* **2003**, *48*, 1511−1524.

(20) Adlhart, C.; Verran, J.; Azevedo, N. F.; Olmez, H.; Keinänen-Toivola, M. M.; Gouveia, I.; Melo, L. F.; Crijns, F. Surface modifications for antimicrobial effects in the healthcare setting: A critical overview. *J. Hosp. Infect.* **2018**, *99*, 239−249.

(21) Monteiro, D. R.; Gorup, L. F.; Takamiya, A. S.; Ruvollo-Filho, A. C.; de Camargo, E. R.; Barbosa, D. B. The growing importance of materials that prevent microbial adhesion: antimicrobial effect of medical devices containing silver. *Int. J. Antimicrob. Agents* **2009**, *34*, 103−110.

(22) Yadav, N.; Dubey, A.; Shukla, S.; Saini, C. P.; Gupta, G.; Priyadarshini, R.; Lochab, B. Graphene oxide-coated surface: inhibition of bacterial biofilm formation due to specific surface−interface interactions. *ACS Omega* **2017**, *2*, 3070−3082.

(23) Zhang, P.; Lin, L.; Zang, D.; Guo, X.; Liu, M. Designing Bioinspired Anti-Biofouling Surfaces based on a Superwettability Strategy. *Small* **2017**, *13*, 1503334.

(24) Pechook, S.; Sudakov, K.; Polishchuk, I.; Ostrov, I.; Zakin, V.; Pokroy, B.; Shemesh, M. Bioinspired passive anti-biofouling surfaces preventing biofilm formation. *J. Mater. Chem. B* **2015**, *3*, 1371−1378.

(25) Pappas, H. C.; Phan, S.; Yoon, S.; Edens, L. E.; Meng, X.; Schanze, K. S.; Whitten, D. G.; Keller, D. J. Self-sterilizing, self-cleaning mixed polymeric multifunctional antimicrobial surfaces. *ACS Appl. Mater. Interfaces* **2015**, *7*, 27632−27638.

(26) Azeredo, J.; et al. Critical review on biofilm methods. *Crit. Rev. Microbiol.* **2017**, *43*, 313−351.

(27) Hannig, C.; Follo, M.; Hellwig, E.; Al-Ahmad, A. Visualization of adherent micro-organisms using different techniques. *J. Med. Microbiol.* **2010**, *59*, 1−7.

(28) Funari, R.; Bhalla, N.; Chu, K.-Y.; Söderström, B.; Shen, A. Q. Nanoplasmonics for real-time and label-free monitoring of microbial biofilm formation. *ACS Sens.* **2018**, *3*, 1499−1509.

(29) Djordjevic, D.; Wiedmann, M.; McLandsborough, L. A. Microtiter plate assay for assessment of Listeria monocytogenes biofilm formation. *Appl. Environ. Microbiol.* **2002**, *68*, 2950−2958.

(30) Ceri, H.; Olson, M. E.; Stremick, C.; Read, R. R.; Morck, D.; Buret, A. The Calgary Biofilm Device: new technology for rapid determination of antibiotic susceptibilities of bacterial biofilms. *J. Clin. Microbiol.* **1999**, *37*, 1771−1776.

(31) Olson, M. E.; Ceri, H.; Morck, D. W.; Buret, A. G.; Read, R. R. Biofilm bacteria: formation and comparative susceptibility to antibiotics. *Can. J. Vet. Res.* **2002**, *66*, 86.

(32) Haagensen, J. A. J.; Klausen, M.; Ernst, R. K.; Miller, S. I.; Folkesson, A.; Tolker-Nielsen, T.; Molin, S. Differentiation and Distribution of Colistin- and Sodium Dodecyl Sulfate-Tolerant Cells in Pseudomonas aeruginosa Biofilms. *J. Bacteriol.* **2007**, *189*, 28−37.

(33) Pousti, M.; Zarabadi, M. P.; Abbaszadeh Amirdehi, M.; Paquet-Mercier, F.; Greener, J. Microfluidic bioanalytical flow cells for biofilm studies: a review. *Analyst* **2019**, *144*, 68−86.

(34) Janakiraman, V.; Englert, D.; Jayaraman, A.; Baskaran, H. Modeling growth and quorum sensing in biofilms grown in microfluidic chambers. *Ann. Biomed. Eng.* **2009**, *37*, 1206−1216.

(35) Ding, Y.; Zhou, Y.; Yao, J.; Xiong, Y.; Zhu, Z.; Yu, X.-Y. Molecular evidence of a toxic effect on a biofilm and its matrix. *Analyst* **2019**, *144*, 2498−2503.

(36) Meyer, M. T.; Roy, V.; Bentley, W. E.; Ghodssi, R. Development and validation of a microfluidic reactor for biofilm monitoring via optical methods. *J. Micromech. Microeng.* **2011**, *21*, 054023.

(37) Nishitani, K.; Sutipornpalangkul, W.; de Mesy Bentley, K. L.; Varrone, J. J.; Bello-Irizarry, S. N.; Ito, H.; Matsuda, S.; Kates, S. L.; Daiss, J. L.; Schwarz, E. M. Quantifying the natural history of biofilm formation in vivo during the establishment of chronic implant-associated Staphylococcus aureus osteomyelitis in mice to identify critical pathogen and host factors. *J. Orthop. Res.* **2015**, *33*, 1311−1319.

(38) Boyd, C. D.; Smith, T. J.; El-Kirat-Chatel, S.; Newell, P. D.; Dufrene, Y. F.; O'Toole, G. A. Structural features of the Pseudomonas fluorescens biofilm adhesin LapA required for LapG-dependent cleavage, biofilm formation, and cell surface localization. *J. Bacteriol.* **2014**, *196*, 2775−2788.

(39) Hannig, C.; Ruggeri, A.; Al-Khayer, B.; Schmitz, P.; Spitzmüller, B.; Deimling, D.; Huber, K.; Hoth-Hannig, W.; Bowen, W. H.; Hannig, M. Electron microscopic detection and activity of glucosyltransferase B, C, and D in the in situ formed pellicle. *Arch. Oral Biol.* **2008**, *53*, 1003−1010.

(40) Sauerbrey, G. The use of quarts oscillators for weighing thin layers and for microweighing. *Z. Phys.* **1959**, *155*, 206−222.

(41) Ballantine, D., Jr.; White, R. M.; Martin, S. J.; Ricco, A. J.; Zellers, E.; Frye, G.; Wohltjen, H. *Acoustic Wave Sensors: Theory, Design and Physico-Chemical Applications*; Elsevier, 1996.

(42) Cho, N.-J.; Kanazawa, K. K.; Glenn, J. S.; Frank, C. W. Employing two different quartz crystal microbalance models to study changes in viscoelastic behavior upon transformation of lipid vesicles to a bilayer on a gold surface. *Anal. Chem.* **2007**, *79*, 7027−7035.

(43) Feng, K.; Li, J.; Jiang, J.-H.; Shen, G.-L.; Yu, R.-Q. QCM detection of DNA targets with single-base mutation based on DNA ligase reaction and biocatalyzed deposition amplification. *Biosens. Bioelectron.* **2007**, *22*, 1651−1657.

(44) Tombelli, S.; Mascini, M.; Turner, A. P. F. Improved procedures for immobilisation of oligonucleotides on gold-coated piezoelectric quartz crystals. *Biosens. Bioelectron.* **2002**, *17*, 929−936.

(45) Funari, R.; Della Ventura, B.; Schiavo, L.; Esposito, R.; Altucci, C.; Velotta, R. Detection of parathion pesticide by quartz crystal microbalance functionalized with UV-activated antibodies. *Anal. Chem.* **2013**, *85*, 6392−6397.

(46) Funari, R.; Della Ventura, B.; Carrieri, R.; Morra, L.; Lahoz, E.; Gesuele, F.; Altucci, C.; Velotta, R. Detection of parathion and patulin by quartz-crystal microbalance functionalized by the photonics immobilization technique. *Biosens. Bioelectron.* **2015**, *67*, 224−229.

(47) Pavey, K. D.; Barnes, L.-M.; Hanlon, G. W.; Olliff, C. J.; Ali, Z.; Paul, F. A rapid, non-destructive method for the determination of Staphylococcus epidermidis adhesion to surfaces using quartz crystal resonant sensor technology. *Lett. Appl. Microbiol.* **2001**, *33*, 344−348.

(48) Heitmann, V.; Wegener, J. Monitoring cell adhesion by piezoresonators: impact of increasing oscillation amplitudes. *Anal. Chem.* **2007**, *79*, 3392−3400.

(49) Chen, M.-Y.; Chen, M.-J.; Lee, P.-F.; Cheng, L.-H.; Huang, L.-J.; Lai, C.-H.; Huang, K.-H. Towards real-time observation of conditioning film and early biofilm formation under laminar flow conditions using a quartz crystal microbalance. *Biochem. Eng. J.* **2010**, *53*, 121−130.

(50) Olsson, A. L. J.; Van der Mei, H. C.; Busscher, H. J.; Sharma, P. K. Influence of cell surface appendages on the bacterium−substratum interface measured real-time using QCM-D. *Langmuir* **2009**, *25*, 1627−1632.

(51) Olsson, A. L. J.; Mitzel, M. R.; Tufenkji, N. QCM-D for non-destructive real-time assessment of Pseudomonas aeruginosa biofilm attachment to the substratum during biofilm growth. *Colloids Surf., B* **2015**, *136*, 928−934.

(52) Kreth, J.; Hagerman, E.; Tam, K.; Merritt, J.; Wong, D. T. W.; Wu, B. M.; Myung, N. V.; Shi, W.; Qi, F. Quantitative analyses of Streptococcus mutans biofilms with quartz crystal microbalance, microjet impingement and confocal microscopy. *Biofilms* **2004**, *1*, 277−284.

(53) Schofield, A. L.; Rudd, T. R.; Martin, D. S.; Fernig, D. G.; Edwards, C. Real-time monitoring of the development and stability of biofilms of Streptococcus mutans using the quartz crystal micro-balance with dissipation monitoring. *Biosens. Bioelectron.* **2007**, *23*, 407−413.

(54) Barrantes, A.; Arnebrant, T.; Lindh, L. Characteristics of saliva films adsorbed onto different dental materials studied by QCM-D. *Colloids Surf., A* **2014**, *442*, 56−62.

(55) Biemmi, E.; Darga, A.; Stock, N.; Bein, T. Direct growth of Cu3 (BTC) 2 (H2O) 3·xH2O thin films on modified QCM-gold electrodes−Water sorption isotherms. *Microporous Mesoporous Mater.* **2008**, *114*, 380−386.

(56) Wang, X.; Cui, F.; Lin, J.; Ding, B.; Yu, J.; Al-Deyab, S. S. Functionalized nanoporous $TiO_2$ fibers on quartz crystal micro-balance platform for formaldehyde sensor. *Sens. Actuators, B* **2012**, *171−172*, 658−665.

(57) Reipa, V.; Almeida, J.; Cole, K. D. Long-term monitoring of biofilm growth and disinfection using a quartz crystal microbalance and reflectance measurements. *J. Microbiol. Methods* **2006**, *66*, 449−459.

(58) Sprung, C.; Wählisch, D.; Hüttl, R.; Seidel, J.; Meyer, A.; Wolf, G. Detection and monitoring of biofilm formation in water treatment systems by quartz crystal microbalance sensors. *Water Sci. Technol.* **2009**, *59*, 543−548.

(59) Amer, M.-A.; Turó, A.; Salazar, J.; Berlanga-Herrera, L.; García-Hernández, M. J.; Chávez, J. A. Multichannel QCM-based system for continuous monitoring of bacterial biofilm growth. *IEEE Trans. Instrum. Meas.* **2019**, 1.

(60) Alexander, T. E.; Lozeau, L. D.; Camesano, T. A. QCM-D Characterization of Time-Dependence of Bacterial Adhesion. *Cell Surf.* **2019**, *5*, 100024.

(61) Drenkard, E. Antimicrobial resistance of Pseudomonas aeruginosa biofilms. *Microbes Infect.* **2003**, *5*, 1213−1219.

(62) Shen, Y.; Stojicic, S.; Haapasalo, M. Antimicrobial efficacy of chlorhexidine against bacteria in biofilms at different stages of development. *J. Endod.* **2011**, *37*, 657−661.

(63) Wang, Z.; Shen, Y.; Haapasalo, M. Effectiveness of endodontic disinfecting solutions against young and old Enterococcus faecalis biofilms in dentin canals. *J. Endod.* **2012**, *38*, 1376−1379.

(64) Guła, G.; Dorotkiewicz-Jach, A.; Korzekwa, K.; Valvano, M. A.; Drulis-Kawa, Z. Complex Signaling Networks Controlling Dynamic Molecular Changes in Pseudomonas aeruginosa Biofilm. *Curr. Med. Chem.* **2019**, *26*, 1979−1993.

(65) Brunette, D. M.; Tengvall, P.; Textor, M.; Thomsen, P. *Titanium in Medicine: Material Science, Surface Science, Engineering, Biological Responses and Medical Applications*; Springer Science & Business Media, 2012.

(66) Wright, C. J.; Shah, M. K.; Powell, L. C.; Armstrong, I. Application of AFM from microbial cell to biofilm. *Scanning* **2010**, *32*, 134−149.

(67) Sule, P.; Wadhawan, T.; Carr, N. J.; Horne, S. M.; Wolfe, A. J.; Prüβ, B. M. A combination of assays reveals biomass differences in biofilms formed byEscherichia colimutants. *Lett. Appl. Microbiol.* **2009**, *49*, 299−304.

(68) Xu, Z.; Liang, Y.; Lin, S.; Chen, D.; Li, B.; Li, L.; Deng, Y. Crystal violet and XTT assays on Staphylococcus aureus biofilm quantification. *Curr. Microbiol.* **2016**, *73*, 474−482.

(69) O'Toole, G. A. Microtiter dish biofilm formation assay. *J. Visualized Exp.* **2011**, *47*, No. e2437.

(70) Feoktistova, M.; Geserick, P.; Leverkus, M. Crystal violet assay for determining viability of cultured cells. *Cold Spring Harb. Protoc.* **2016**, *2016*, pdb.prot087379.